

**Table III.** Average Values for the Exchange Links Corresponding to Different Iron Sites in  $\text{Fe}_2(\text{MoO}_4)_3$ 

	site no.			
	1	2	3	4
pathway, Å	7.488	7.497	7.486	7.475
Fe-O-Mo, deg	149.7	147.5	150.7	153.2

shorter is the total pathway, the closer is the O-Mo-O angle to that of a regular tetrahedron, and the closer are the Fe-O-Mo angles to 180°. Because the distortions of ( $\text{FeO}_6$ ) octahedra and ( $\text{MoO}_4$ ) tetrahedra are very small, the exchange interaction is likely to depend mostly on the Fe-O-Mo angles, which vary in the range 133.2–167.6°. It appears from the comparison of mean angles and lengths of pathways (see Table III) that site 4 is likely to correspond to sextuplet  $\beta$ . From the value for quadrupole splitting in the paramagnetic state  $\Delta_{\text{obsd}} = 0.20 \text{ mm}\cdot\text{s}^{-1}$ ,  $\eta_{\text{calcd}} = 0.36$ , and the orientation of the

principal axes of the EFG tensor for site 4 (Table I), the quadrupole perturbation has been calculated for possible orientations of the magnetic axis and compared with the experimental value  $\epsilon = 0.00 \pm 0.02 \text{ mm}\cdot\text{s}^{-1}$ . The results suggest that the magnetic moments lie in the  $ac$  plane, making an angle of 37–58 or 122–143° with the  $c$  axis as the most plausible solution.

It is worth emphasizing that the latter result relies on many hypotheses and that a neutron diffraction investigation should be undertaken in order to determine the magnetic structure unambiguously.

**Acknowledgment.** The present work has been performed with the financial support of Rhône-Poulenc SA. The authors wish to thank B. Chevalier, who carried out the X-ray diffraction experiments at 4.2 K and Professor R. Georges for helpful discussions.

**Registry No.**  $\text{Fe}_2\text{Mo}_3\text{O}_{12}$ , 13769-81-8.

Contribution from the Inorganic Chemistry Laboratory, Oxford University, Oxford OX1 3QR, England, the Chemical Crystallography Laboratory, Oxford University, Oxford OX1 3PD, England, the Department of Chemistry, University of Missouri—Rolla, Rolla, Missouri 65401, and the Nuclear Physics Division, Atomic Energy Research Establishment, Harwell, Didcot OX11 0RA, England

## Study of the Magnetic Properties of Iron(III) Molybdate, by Susceptibility, Mössbauer, and Neutron Diffraction Techniques

PETER D. BATTLE,\*<sup>1a</sup> ANTHONY K. CHEETHAM,<sup>1b</sup> GARY J. LONG,\*<sup>1c,d</sup> and GEOFFREY LONGWORTH<sup>1d</sup>

Received November 23, 1981

A powder neutron diffraction study and subsequent line-profile analysis of the magnetic structure of iron(III) molybdate at 2 K indicate that it is a four-sublattice antiferromagnet containing four crystallographically distinct iron atoms in the space group  $P2_1/a$  ( $b$  unique). The results also confirm that the 2 K nuclear structure is the same as that found at room temperature by single-crystal X-ray diffraction. An analysis of covalency in iron(III) molybdate reveals a higher degree of covalency ( $A_o^2 + 2A_x^2 + A_s^2 = 9.15\%$ ) in the iron(III) to oxygen bonds than is found in the structurally related iron(III) sulfate (6.1%). A Mössbauer-effect study indicates that, at 11.8 K and above, iron(III) molybdate is paramagnetic with parameters typical of an octahedral high-spin iron(III) compound. Between 11.72 and 11.59 K both ordered and paramagnetic phases coexist. Below 11.72 K the Mössbauer spectrum shows the presence of spontaneous magnetic ordering with four inequivalent magnetic hyperfine fields. On three of the iron sites, the hyperfine fields are rather similar while the fourth site exhibits a significantly greater hyperfine field. The differences between various combinations of the four hyperfine fields show maxima at about 10 K. At 1.14 K the field values are 540, 529, 519, and 509 kOe. The isomer shifts for each site are similar at ca. 0.52 mm/s, and the quadrupole shifts are small at ca.  $\pm 0.01$  mm/s. Magnetic susceptibility studies confirm that the material is paramagnetic above ca. 20 K, with an effective magnetic moment of  $5.92 \mu_B$  and a Curie-Weiss temperature of  $-55.6$  K. The magnetic susceptibility shows a peak of ca. 10 K, the magnitude of which increases with decreasing applied field between 45.81 and 9.95 kG. The magnetization data also indicate spontaneous ferrimagnetic ordering for iron(III) molybdate below ca. 14 K with a maximum in the spontaneous moment between 9 and 10 K. This behavior confirms that, below ca. 20 K, iron(III) molybdate is a weak L-type ferrimagnet. At temperatures below 6 K, the magnetic susceptibility increases at high applied fields, indicating the presence of a spin-flop transition with a critical field of ca. 20 kG at 4.2 K.

### Introduction

We have previously published<sup>2</sup> a study of monoclinic, anhydrous iron(III) sulfate,  $\text{Fe}_2(\text{SO}_4)_3$ , which shows novel ferrimagnetic ordering arising from the presence of two crystallographically distinct octahedral iron(III) sites. The results provided a prescription for identifying materials with similar properties, and we have now completed a detailed investigation of the magnetic properties of the structurally related iron(III) molybdate,  $\text{Fe}_2(\text{MoO}_4)_3$ .

Iron(III) molybdate is chemically isostructural with iron(III) sulfate,<sup>2,3</sup> the structure consisting of an infinite network of iron-oxygen-molybdenum linkages in which the oxygen atoms coordinate the iron atoms octahedrally and the molybdenum atoms tetrahedrally; the octahedra share corners with the tetrahedra. However, there is an important crystallographic difference between the structures in that there are either four<sup>3</sup> or eight<sup>4</sup> distinct iron(III) sites in the molybdate and the unit cell has twice the volume of that of the sulfate, which contains only two iron(III) sites. The structure of the molybdate, as determined by Chen,<sup>3</sup> is presented in Figure 1. The uncertainty concerning the number of iron(III) sites arises because

(1) (a) Inorganic Chemistry Laboratory, Oxford University. (b) Chemical Crystallography Laboratory, Oxford University. (c) University of Missouri—Rolla. Address correspondence to G.J.L. at this address. (d) Atomic Energy Research Establishment.  
(2) Long, G. J.; Longworth, G.; Battle, P.; Cheetham, A. K.; Thundathil, R. V.; Beveridge, D. *Inorg. Chem.* 1979, 18, 624.

(3) Chen, H. *Mater. Res. Bull.* 1979, 14, 1583.

(4) Rapposch, M. H.; Anderson, J. B.; Kostiner, E. *Inorg. Chem.* 1980, 19, 3531.

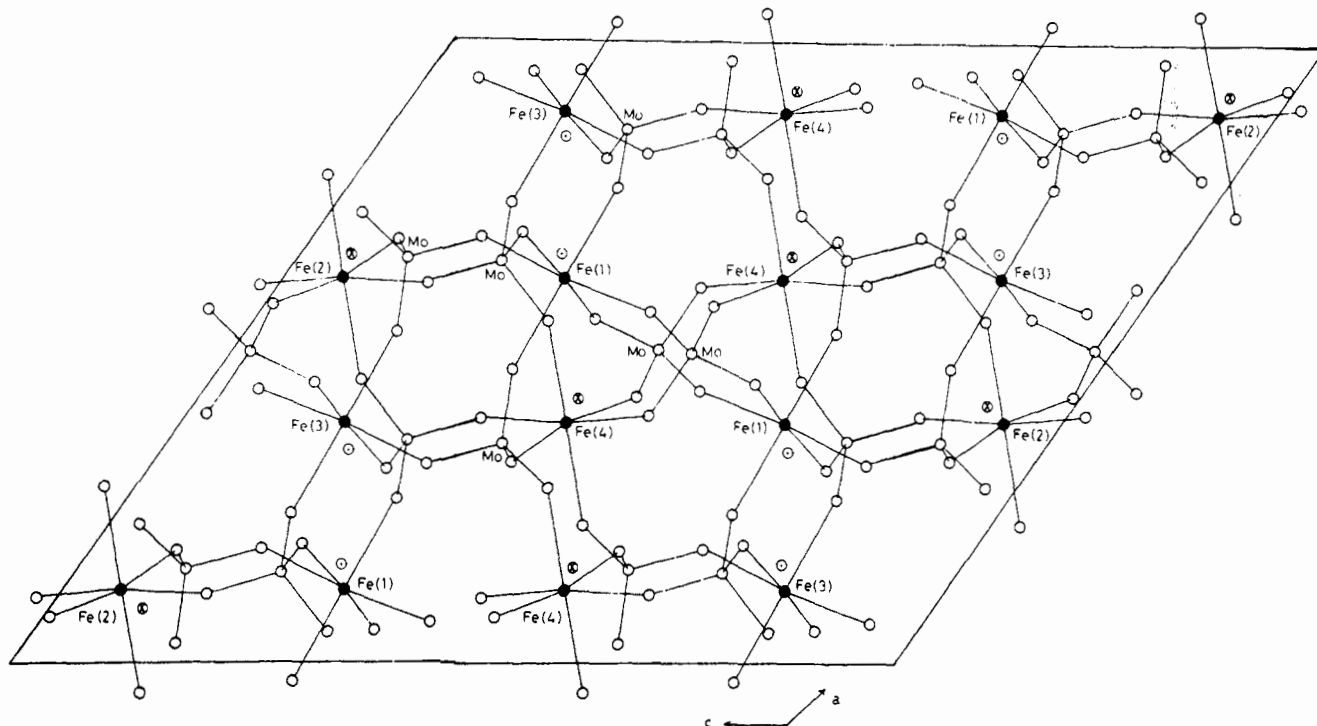


**Figure 1.** Unit cell of the iron(III) molybdate structure. The magnetic vectors are represented by  $\oplus$  and  $\ominus$  for moments oriented in the  $+b$  and  $-b$  directions, respectively.

it is not clear from single-crystal X-ray studies<sup>3,4</sup> whether the material is truly noncentrosymmetric or whether it appears to be so because of twinning. The similarity between the iron(III) environments has been demonstrated in a room-temperature Mössbauer-effect study<sup>5</sup> in which the spectrum consisted of one broad doublet comprising four (or eight) superimposed, quadrupole-split iron(III) lines. The molybdate is thus a system where we might expect magnetic interactions similar to those found in iron(III) sulfate, with added subtleties brought about by the increased number of distinct iron(III) sites. A high-temperature study<sup>4</sup> of the magnetic susceptibility of iron(III) molybdate, in which a Curie-Weiss temperature of  $-62.7$  K is reported, has indicated that antiferromagnetic ordering can be anticipated at low temperatures. It should be noted that, in addition to the above interest, iron(III) molybdate is important as a selective oxidation catalyst and is used to convert methanol to formaldehyde.<sup>6</sup>

### Experimental Section

Iron(III) molybdate was prepared by firing a well-ground, pelleted stoichiometric mixture of Specpure iron(III) oxide, obtained from Johnson Matthey Chemicals, and AnalaR molybdenum trioxide, obtained from BDH, for 24 h at  $700$  °C in a platinum crucible. The sample was then annealed for 19 h at  $400$  °C to ensure that only the low-temperature monoclinic phase was present.<sup>7</sup> The X-ray powder diffraction pattern of the product was in good agreement with those reported by previous workers.<sup>8,9</sup> Analytical electron microscopy indicated excellent sample homogeneity. Iron and molybdenum were determined by atomic absorption. Anal. Calcd for  $\text{Fe}_2\text{Mo}_3\text{O}_{12}$ : Fe, 18.8; Mo, 48.6. Found: Fe, 18.3; Mo, 48.3.

Powder neutron diffraction data were collected on the D1A powder diffractometer at the Institut Laue Langevin, Grenoble, France. Neutrons with a mean wavelength of  $1.905$  Å were used to obtain data in the angular range  $6^\circ < 2\theta < 93.5^\circ$ , the sample being held

in a helium cryostat at a temperature of 2 K. The experiment was then repeated at room temperature.

The magnetic susceptibility of a polycrystalline sample was measured between 4.2 and 80 K by using an Oxford Instruments Faraday balance, calibrated with  $\text{CuSO}_4 \cdot 5\text{H}_2\text{O}$ . Temperatures were measured with a gold (0.03% iron) vs. chromel thermocouple with its reference junction in the liquid-helium bath. The susceptibility was measured in six fields up to 45.81 kG with a maximum applied gradient of  $122$  G  $\text{cm}^{-1}$ .

The Mössbauer spectra were obtained on a Harwell constant-acceleration spectrometer by using a room-temperature rhodium-matrix source and calibrating with natural  $\alpha$ -iron foil. The 4.2 K and lower temperature spectra were measured in a cryostat in which the sample was placed directly in liquid helium. The sample temperature was determined by measuring the vapor pressure above the liquid helium. Temperatures between 4.2 and 78 K were obtained through the use of a variable-temperature insert placed in the liquid-helium cryostat. The temperature was measured by a gold-iron thermocouple and was controlled to ca.  $\pm 0.03$  K. The Mössbauer spectra were evaluated by using least-squares minimization computer programs and the Harwell IBM 370/168 computer facilities. The isomer shift and quadrupole splitting and shift values are accurate to ca.  $\pm 0.02$  mm/s and the hyperfine fields are accurate to ca.  $\pm 5$  kOe.

### Results

**Neutron Diffraction Results.** The 2 K powder neutron diffraction pattern was indexed in the centrosymmetric space group  $P2_1/a$  ( $b$  unique) as used by Chen.<sup>3</sup> There was no evidence to suggest the noncentrosymmetric space group  $P2_1$ .<sup>4</sup> The refined cell parameters are  $a = 15.637$  (3) Å,  $b = 9.224$  (3) Å,  $c = 18.173$  (3) Å, and  $\beta = 125.26$  (1)°. The numbers in parentheses here and elsewhere in this paper indicate the estimated standard deviations in the least significant digits. In this case they do not include any allowance for error in the estimation of the neutron wavelength.

The peak intensities in the pattern clearly indicated that the sample was magnetically ordered at 2 K. The low-temperature magnetic structure was refined by the Rietveld profile analysis technique,<sup>10</sup> the data with  $2\theta < 16^\circ$  being discarded because of problems with asymmetric peak shapes.<sup>2</sup> The remaining

(5) Herzenberg, C. L.; Riley, D. L. *J. Phys. Chem. Solids* **1969**, *30*, 2108.

(6) Popov, B. I.; Sedova, L. L.; Kustova, G. N.; Plysova, L. M.; Maksimov, Yu. V.; Matveev, A. I. *React. Kinet. Catal. Lett.* **1976**, *5*, 43.

(7) Sleight, A. W.; Brixner, L. H. *J. Solid State Chem.* **1973**, *7*, 172.

(8) Massarotti, V.; Flor, G.; Marini, A. *J. Appl. Crystallogr.* **1981**, *14*, 64.

(9) Klevsov, P. V.; Klevtsova, R. F.; Kefeli, L. M.; Plysova, L. M. *Inorg. Mater. (Engl. Transl.)* **1965**, *1*, 843; *Izv. Akad. Nauk SSR, Neorg. Mater.* **1965**, *1*, 918.

(10) Rietveld, H. M. *J. Appl. Crystallogr.* **1969**, *2*, 65.

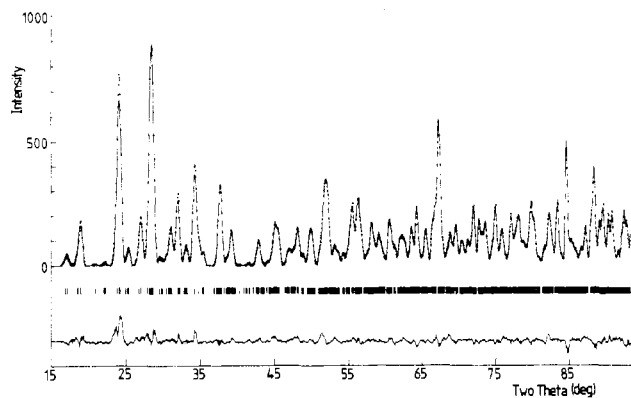


Figure 2. Observed, calculated, and difference profiles for the powder neutron diffraction pattern of iron(III) molybdate at 2 K.

1549 observed profile points in the data set were distributed over 994 reflections. The atomic coordinates determined by Chen<sup>3</sup> at room temperature were used in all our refinements, there being insufficient data in the profile to permit variation of the 102 additional parameters necessary for a full structure refinement. We have thus essentially solved and refined the magnetic structure against the background of an assumed crystal structure.<sup>3</sup> The overall isotropic temperature factor was held constant at  $0.02 \text{ \AA}^2$  to further simplify the problem. This was the value found, after refinement, for the isostructural iron(III) sulfate at 4.2 K. The following neutron scattering lengths were used:<sup>11</sup>  $b_{\text{Fe}} = 0.95$ ,  $b_{\text{Mo}} = 0.69$ ,  $b_{\text{O}} = 0.58$  ( $\times 10^{-14}$  m). The iron(III) free-ion form factor was used<sup>12</sup> in refining the magnetic structure. The magnetic structure of iron(III) sulfate led us to predict that the magnetic ordering in iron(III) molybdate would be as follows: Fe(1) and Fe(3) to have parallel spins; Fe(2) and Fe(4) to have parallel spins that are antiparallel to Fe(1) and Fe(3). The ordering on each of the four iron sublattices should be ferromagnetic. In this way the number of antiferromagnetically coupled nearest neighbors around each iron(III) is maximized at 12. The designation of each of the four sublattices is taken from ref 3. This was the first model used for the magnetic structure, and because it was successful, no alternatives were tried. The final step was the refinement of the direction and magnitude of the iron(III) magnetic moments, and the best fit was obtained with a moment of  $4.34$  ( $3$ )  $\mu_{\text{B}}$  per iron(III) aligned along the crystallographic  $b$  axis. The final weighted profile  $R$  value was 8.9%, and the observed and calculated diffraction profiles are shown in Figure 2. The largest deviations revealed in the difference plot in this figure are also found in the data collected at room temperature and are therefore not magnetic in origin, but attempts to explain them in terms of preferred orientation were unsuccessful. They may stem from uncertainties in the oxygen coordinates determined in the single-crystal X-ray study by Chen.<sup>3</sup>

A quantitative measure of the degree of covalency present about an octahedrally coordinated  $d^5$  ion can be calculated from eq 1, which has been derived from a molecular orbital

$$S/S_0 = 1 - 1.2(A_\sigma^2 + 2A_\pi^2 + A_s^2) \quad (1)$$

description of the bonding.<sup>13</sup> In this expression  $S$  is the measured spin,  $S_0$  is the free-ion spin corrected for zero-point spin deviation, and the  $A_i$  values are the  $\sigma$ ,  $\pi$ , and  $s$  covalency parameters. The magnitude of the zero-point spin deviation depends upon the structure type, and we have used the same estimated value of 2.5% as in our earlier work on iron(III)

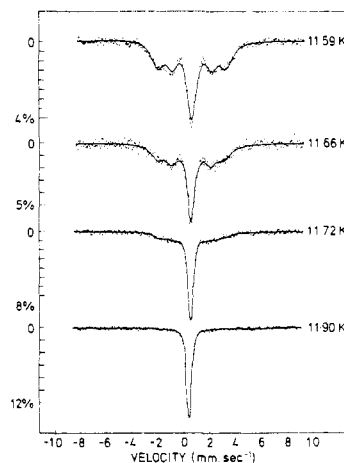


Figure 3. Mössbauer-effect spectra of iron(III) molybdate obtained between 11.90 and 11.59 K.

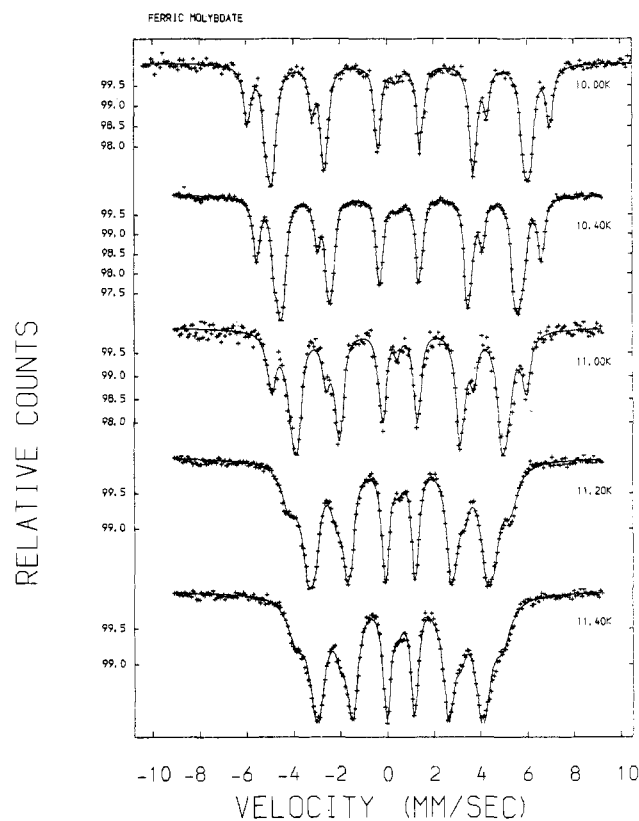


Figure 4. Mössbauer-effect spectra of iron(III) molybdate obtained between 11.4 and 10.0 K.

Table I. Mössbauer-Effect Parameters for Iron(III) Molybdate—Paramagnetic Phase<sup>a</sup>

$T$ , K	$\delta$	$\Delta E_Q$	$\Gamma_{1/2}$	% area	$\chi^2$
11.59	0.53	0.24	0.57	24	1.5
11.66	0.51	0.20	0.44	29	1.1
11.72	0.52	0.20	0.36	55	1.1
11.9	0.52	0.20	0.30	100	0.8
12.2	0.52	0.20	0.30	100	0.9
13.2	0.52	0.20	0.30	100	1.0
78	0.52	0.19	0.29	100	1.1
298	0.42	0.18	0.27	100	1.1

<sup>a</sup> All data in mm/s relative to natural  $\alpha$ -iron foil.

sulfate. The covalency parameter sum for iron(III) molybdate is calculated as  $A_\sigma^2 + 2A_\pi^2 + A_s^2 = 9.15$  (1.0)%.

**Mössbauer-Effect Results.** The Mössbauer spectra of iron(III) molybdate are presented in Figures 3–5. The spectra

(11) Bacon, G. E. *Acta Crystallogr., Sect. A* 1972, A28, 357.

(12) Watson, R. E.; Freeman, A. J. *Acta Crystallogr.* 1961, 14, 27.

(13) Hubbard, J.; Marshall, W. *Proc. Phys. Soc., London* 1965, 86, 561.

Table II. Mössbauer-Effect Parameters for Iron(III) Molybdate—Magnetic Phase<sup>a</sup>

T, K	Fe site a			Fe site b			Fe site c			Fe site d			singlet		
	$H_{int}$	$\delta$	QS	$H_{int}$	$\delta$	QS	$H_{int}$	$\delta$	QS	$H_{int}$	$\delta$	QS	$\delta$	% area	$\chi^2$
1.14	529	0.575	0.057	519	0.495	-0.023	508	0.554	0.035	541	0.516	-0.003	...	...	2.8
4.2	507	0.519	0.010	501	0.529	-0.013	493	0.520	0.001	526	0.518	0.014	0.394	2	3.3
6.0	476	0.537	0.006	475	0.523	-0.003	467	0.524	0.005	509	0.522	0.014	0.423	2	1.3
8.0	426	0.537	0.002	420	0.517	-0.017	412	0.532	0.009	470	0.523	0.011	0.378	2	1.1
9.0	400	0.528	-0.010	391	0.528	-0.006	382	0.528	0.008	447	0.521	0.013	0.395	2	1.7
10.0	351	0.525	0.004	339	0.530	0.009	331	0.522	0.010	400	0.529	0.014	0.389	2	1.0
10.4	330	0.528	0.001	316	0.517	-0.008	305	0.524	0.015	377	0.525	0.014	0.399	2	1.4
11.0	288	0.523	0.004	280	0.521	-0.002	268	0.527	0.010	337	0.517	0.013	0.423	2	1.5
11.2	247	0.538	-0.011	242	0.520	0.003	225	0.527	0.008	293	0.532	0.013	0.457	2	1.4
11.4	232	0.536	0.005	226	0.520	0.009	210	0.525	0.008	275	0.518	0.024	0.426	3	1.5
11.59 <sup>b</sup>										164	0.51	...			1.5
11.66 <sup>c</sup>										159	0.47	...			1.1
11.72 <sup>d</sup>										148	0.56	...			1.1

<sup>a</sup> All data in mm/s (or kOe for the  $H_{int}$ ) are relative to natural  $\alpha$ -iron foil. The four magnetic site ratios are fixed at unity, and their relative components are 3:x:1:1:x:3 with x values of ca. 2.0. <sup>b</sup> Relative area of 76%. <sup>c</sup> Relative area of 71%. <sup>d</sup> Relative area of 45%.

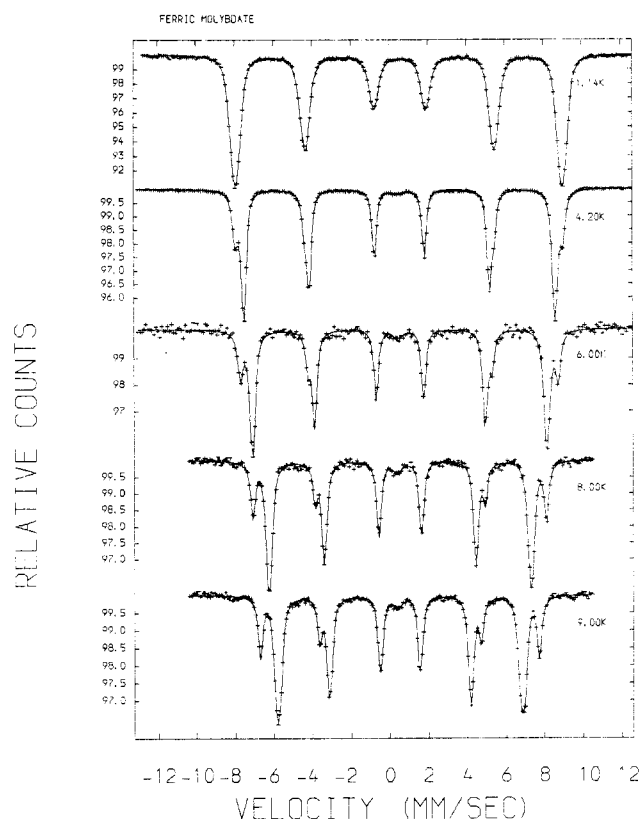


Figure 5. Mössbauer-effect spectra of iron(III) molybdate obtained between 9.0 and 1.14 K.

reveal that iron(III) molybdate is paramagnetic at 11.90 K and above. Higher temperature spectra closely resemble that shown at 11.90 K in Figure 3, except that a small quadrupole splitting is apparent in the expanded spectra. The Mössbauer spectral parameters in the paramagnetic phase are presented in Table I. These parameters represent the average for the four crystallographically distinct iron(III) sites, each of which is so similar that no resolution of the individual components is possible in the paramagnetic phase. The room-temperature Mössbauer spectral parameters are very similar to those reported earlier by Herzenberg and Riley.<sup>5</sup>

Iron(III) molybdate shows the first evidence for long-range magnetic correlation at 11.72 K (see Figure 3), and both the paramagnetic and ordered phases coexist between 11.72 and 11.59 K. The Mössbauer spectral parameters for the magnetically ordered phase are presented in Table II. The spectra for the ordered phase have been fitted by using the following

models. For temperatures between 1.14 and 11.4 K, four magnetic sextets were fitted, with relative areas of 1:1:1:1, each sextet having relative component intensities of 3:x:1:1:x:3. The value of x was found to be close to 2.0. In addition, for the spectra at temperatures between 4.2 and 11.4 K an additional singlet was included at ca. 0.4 mm/s. The fits resulting from this model are shown in Figures 4 and 5, and the hyperfine parameters are presented in Table II. For the spectra obtained at 11.59, 11.66, and 11.72 K, only one magnetic component could be identified (see Figure 3). The temperature dependence of the magnetic hyperfine fields are presented in Figure 6A. The differences between various hyperfine fields are plotted in Figure 6B. The maxima are observed at ca. 9–10 K. The singlet observed at ca. 0.4 mm/s between 11.4 and 4.2 K is an impurity line that represents ca. 2% of the total Mössbauer absorption and is apparently ordered at 1.14 K. At this time we are not certain of the nature of this impurity but note that it might be a superparamagnetic material containing iron(III).

**Magnetic Susceptibility Results.** The low-temperature molar magnetic susceptibility of iron(III) molybdate is plotted in Figure 7 for six different applied fields. Below ca. 15 K the susceptibility deviates from Curie–Weiss behavior, reaching a maximum at ca. 10 K. The exact temperature of the maximum is a function of applied field, varying from 9.6 K in an applied field of 9.95 kG to 10.3 K in a field of 45.81 kG. The magnitude of the susceptibility maximum decreases as the applied field is increased. Figure 8A shows the variation of the magnetization with applied field for a number of temperatures and Figure 8B shows the temperature dependence of the spontaneous magnetization. In fields of 20 kG and greater there is an increase in the susceptibility at low temperatures; the temperature at which the susceptibility starts to rise increases with increasing applied field. A complete set of susceptibility data is presented in Table III.<sup>14</sup>

Magnetic susceptibility data in the range of 25–80 K show Curie–Weiss behavior with a  $\Theta$  of -55.6 K and a  $\mu_{eff}$  of 5.92 (10)  $\mu_B$ . This moment is in good agreement with that measured in iron(III) sulfate<sup>2</sup> (5.85  $\mu_B$ ) but it is considerably larger than the value of 5.5  $\mu_B$  reported previously<sup>4</sup> for iron(III) molybdate.

#### Discussion

The results of our experiments clearly demonstrate that iron(III) molybdate is an L-type ferrimagnet<sup>15</sup> whose behavior is very similar to that of iron(III) sulfate.<sup>2</sup> The low-temperature Mössbauer data are consistent with the presence of

(14) Table III may be found in the supplementary material.

(15) Néel, L. *Ann. Phys. (Paris)* **1948**, [12] 3, 137.

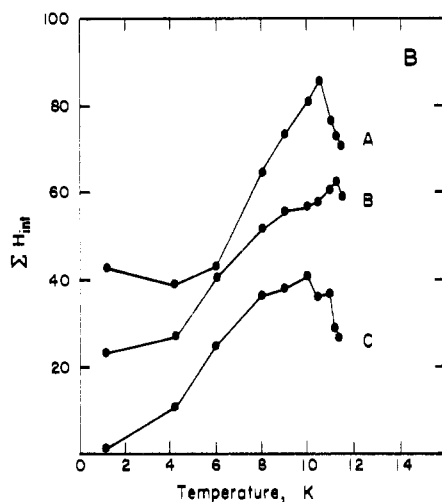
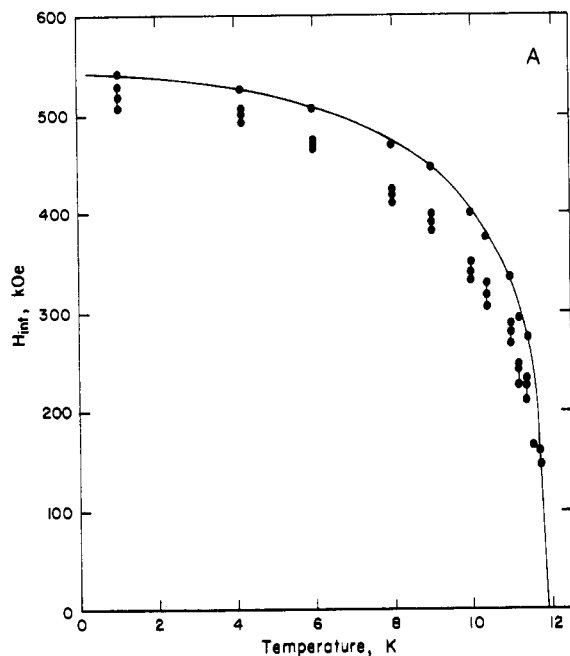


**Figure 6.** Plot of the internal hyperfine fields (see text) on each sublattice (A) and differences between the possible combinations of these fields,  $\Sigma H_{int}$ , as functions of temperature (B). The sum of the internal hyperfine fields is  $H_a + H_d - H_b - H_c$  for curve A,  $H_b + H_d - H_a - H_c$  for curve B, and  $H_c + H_d - H_a - H_b$  for curve C.

four crystallographically different iron(III) sites (designated Fe(1)–Fe(4)) compared with two (Fe(1) and Fe(2)) in the sulfate. However, the ordering pattern of the spins in the molybdate is essentially identical with that in the sulfate. Fe(1) and Fe(3), which correspond to Fe(1) in the sulfate, are aligned antiparallel to Fe(2) and Fe(4), which correspond to Fe(2) in the sulfate. From this we may conclude that the antiferromagnetic exchange pathways are essentially the same in the two compounds. The spin directions in the two materials are, however, orthogonal, being along the *b* axis in the molybdate and in the *ac* plane of the sulfate. The magnetic anisotropy in high-spin  $d^5$  compounds is expected to be determined by the weak dipole–dipole interactions,<sup>16</sup> and it is not surprising that differences in the cation–cation distances between the two compounds are sufficient to produce alternative spin directions.

It is instructive to consider the low-temperature Mössbauer data and susceptibility results together. The first sign of magnetic ordering is apparent in the Mössbauer spectrum at

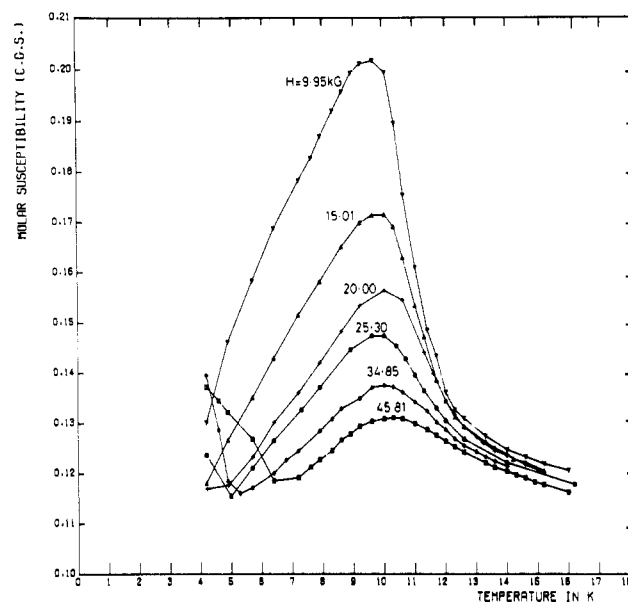


**Figure 7.** Molar magnetic susceptibility of iron(III) molybdate vs. temperature for the indicated applied fields.

11.72 K, and at 11.4 K there appears to be no residual paramagnetic signal (excepting the weak impurity line referred to above). As the sample is cooled between 11.4 and 4.2 K, it is apparent that there are two main sets of six lines. These lines correspond to the magnetic hyperfine fields of the four iron sites, three of which are sufficiently close that their components are not visually resolved. At 1.14 K, the hyperfine field of the outer line appears to be virtually saturated at 541 kOe, and the average field for the other three sites is 519 kOe. The magnetic susceptibility measurements at an applied field of 10 kG show a pronounced peak with a maximum at 9.6 K (Figure 7). Our rationalization of this behavior is essentially the same as for that in the sulfate. In the temperature range 11.4–4.2 K, the sublattice magnetizations saturate at slightly different rates. The peak in the susceptibility curve corresponds to the imbalance between the net sublattice magnetizations of Fe(1) and Fe(3) compared to those of Fe(2) and Fe(4). This imbalance results in a net ferrimagnetic interaction and to the spontaneous magnetization illustrated in Figure 8. The maximum ferrimagnetic contribution to the susceptibility occurs at ca. 10 K, and the temperature of this maximum is slightly field dependent. The Mössbauer-effect spectra reveal this ferrimagnetic behavior through the differences in the magnetic hyperfine field of the four iron sites. Figure 6B indicates that the maximum difference in the hyperfine fields also occurs at ca. 10 K. It should be noted that the peaks in the magnetic susceptibility (Figure 7), spontaneous magnetization (Figure 8B), and  $\Delta H_{int}$  need not occur at exactly the same temperature. The susceptibility and spontaneous magnetization peaks are determined in the presence of an external field, whereas the  $\Delta H_{int}$  is obtained in the absence of any applied field. Because at each temperature the hyperfine field is expected to be proportional to the spontaneous magnetization, it should be possible to produce a curve similar in form to that of the magnetization (see below) by taking differences in field values, e.g.,  $H_a + H_b - H_c - H_d$ , etc., and hence relating the spin directions to the particular iron sites. If this is done, only one curve, C, tends toward  $\Sigma H_{int} = 0$  at absolute zero, as required by the magnetic susceptibility results.

The influence of an applied field on the magnetic susceptibility peak is particularly interesting. The peak in the susceptibility is depressed and the maximum shifts to higher temperatures as the field is increased. It seems likely that the applied field brings all the iron sublattices closer to saturation.

(16) Keffer, F.; O'Sullivan, W. *Phys. Rev.* **1957**, *108*, 637.

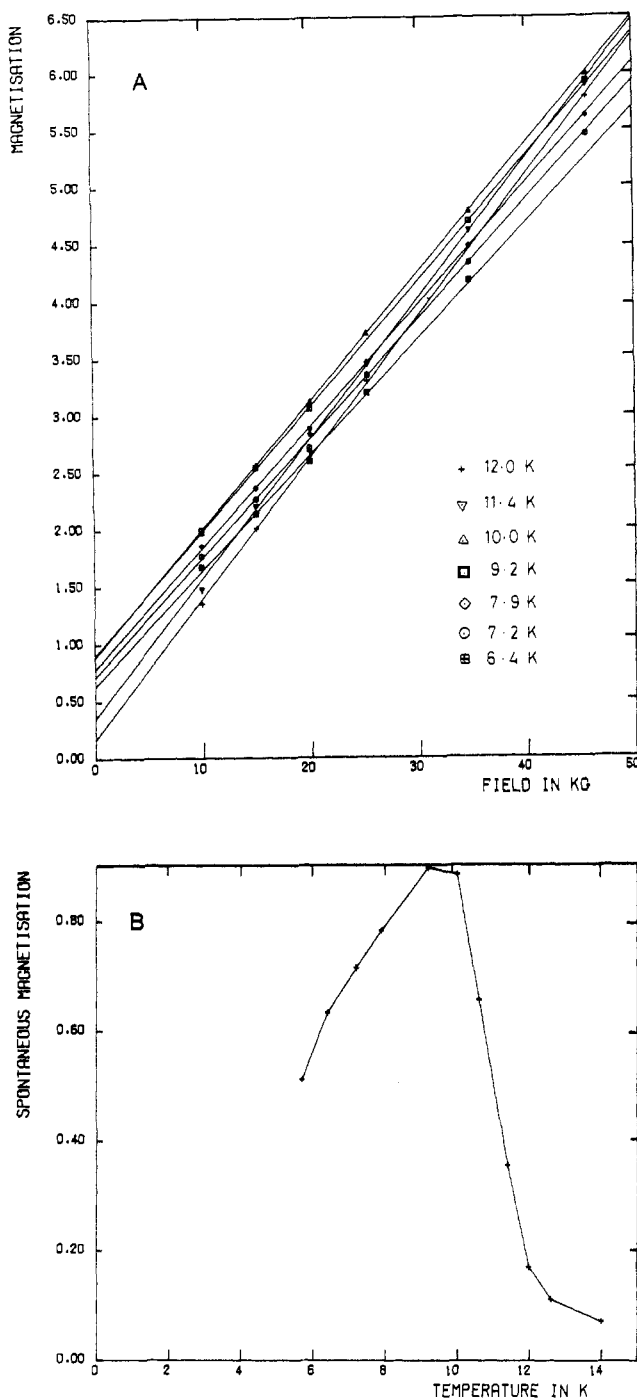


Figure 8. Magnetization of iron(III) molybdate vs. applied field (A) and spontaneous magnetization vs. temperature (B).

The effect is more pronounced for the three sites with the lower magnetization, and hence the magnetic behavior tends toward that of a normal antiferromagnet in the larger fields. The cancellation of sublattice magnetizations is therefore more complete, leading to a diminution of the magnetic susceptibility peak and a shift of its maximum toward the temperature at which magnetic ordering is first observed, i.e.,  $T_N$ . The increase in susceptibility at ca. 6 K, which is only observed in applied fields of 20 kG and above, may be attributed to a spin-flop transition. Mössbauer-effect studies at 4.2 K de-

tected a spin-flop transition in iron(III) sulfate,<sup>2</sup> at a critical field between 10 and 30 kG. The critical fields thus appear to be of similar magnitudes in the two compounds. The nature of this transition is currently subject to further investigation.

The relative Néel temperatures of the molybdate (11.72 K) and the sulfate (28.8 K) are consistent with both longer exchange pathways in the former compound and the greater covalency in the sulfate anion. This trend is also reflected in the Curie-Weiss values of  $-55.6$  and  $-82.0$  K for the iron(III) molybdate and iron(III) sulfate, respectively.

The neutron and Mössbauer results enable us to discuss the bonding in iron(III) molybdate and to compare it with that in iron(III) sulfate. All the data are consistent with a higher degree of covalency in the iron-oxygen bonds of the molybdate than in the sulfate. The most direct evidence for this is to be found in the magnitude of the iron(III) moments determined by neutron diffraction; these yield covalency sums of 9.15 (1.00%) and 6.1 (1.4%) for the molybdate and sulfate, respectively. The values are, however, smaller than those observed in mixed-metal oxides of iron(III), for example,  $\text{Sr}_2\text{-Fe}_2\text{O}_3$  (15.3%),<sup>17</sup>  $\text{LaFeO}_3$  (10.0%), and  $\text{YFeO}_3$  (11.0%).<sup>18</sup> The formal charge on oxygen is larger in the mixed oxides than it is in the molybdate and sulfate, thus leading to higher covalency. The Mössbauer hyperfine field data also support the proposal of higher covalency in the molybdate, the values at saturation being ca. 541 and ca. 550 kOe for the molybdate and sulfate, respectively. These values are determined by the magnitude of the spin at the Fe(III) sites.<sup>19</sup> The last and possibly most informative indication of greater covalency in the molybdate emerges from the Mössbauer isomer shift data. At 4.2 K the average value of the isomer shift in the molybdate is ca. 0.53 mm/s compared with 0.58 mm/s in the sulfate. This implies a greater s-electron density at the iron nucleus in the molybdate, suggesting that ligand to metal 4s-orbital donation is an important covalent interaction. It should be noted that the neutron experiment alone does not differentiate between the different covalent interactions. If the isomer shift had increased, it would have represented a decrease in s-electron density at the nucleus, probably caused by more effective shielding produced from ligand to metal 3d-orbital covalency. The greater covalency in the molybdate is not expected. It presumably stems from the greater electron density on oxygen in the molybdate ion as a consequence of the lower electronegativity of molybdenum when compared with sulfur.

**Acknowledgment.** We thank A. Hewat and S. Heathman at the ILL and B. J. Laundry and L. Becker at AERE Harwell for their assistance during the course of this work. P.D.B. is grateful to the Central Electricity Generating Board and St. Catherine's College, Oxford, for the award of a research fellowship, and we wish to thank NATO for a cooperative scientific research grant, No. 217.80.

**Registry No.**  $\text{Fe}_2\text{Mo}_3\text{O}_{12}$ , 13769-81-8.

**Supplementary Material Available:** Table III, listing molar magnetic susceptibility data for iron(III) molybdate (1 page). Ordering information is given on any current masthead page.

(17) Greaves, C.; Jacobson, A. J.; Tofield, B. C.; Fender, B. E. F. *Acta Crystallogr., Sect. B*, **1975**, *B31*, 641.

(18) Tofield, B. C.; Fender, B. E. F. *J. Phys. Chem. Solids*, **1970**, *31*, 2741.

(19) Sawatzky, G. A.; van der Woude, F. J. *J. Phys., Colloque (Orsay, Fr.)* **1974**, *35* (C-6), 47.